

Robust estimation of tear film surface quality in lateral shearing interferometry

Dorota H. Szczesna

Wroclaw University of Technology
Institute of Physics
Wybrzeze Wyspianskiego 27
Wroclaw, 50-370
Poland

and
Queensland University of Technology
School of Optometry
Victoria Park Road, Kelvin Grove
Brisbane, Queensland 4059
Australia

D. Robert Iskander

Queensland University of Technology
School of Optometry
Victoria Park Road, Kelvin Grove
Brisbane, Queensland 4059
Australia

Abstract. Interferometry is a sensitive technique for recording tear film surface irregularities in a noninvasive manner. At the same time, the technique is hindered by natural eye movements resulting in measurement noise. Estimating tear film surface quality from interferograms can be reduced to a spatial-average-localized weighted estimate of the first harmonic of the interference fringes. However, previously reported estimation techniques proved to perform poorly in cases where the pattern fringes were significantly disturbed. This can occur in cases of measuring tear film surface quality on a contact lens on the eye or in a dry eye. We present a new estimation technique for extracting the first harmonic from the interference fringes that combines the traditional spectral estimation techniques with morphological image processing techniques. The proposed technique proves to be more robust to changes in interference fringes caused by natural eye movements and the degree of dryness of the contact lens and corneal surfaces than its predecessors, resulting in tear film surface quality estimates that are less noisy. © 2009 Society of Photo-Optical Instrumentation Engineers. [DOI: 10.1117/1.3275474]

Keywords: tear film stability; dry eye; spectral analysis; image processing.

Paper 09357R received Aug. 14, 2009; revised manuscript received Oct. 12, 2009; accepted for publication Oct. 20, 2009; published online Dec. 28, 2009.

1 Introduction

One of the most common eye health problems in the older population is dry eye syndrome. The condition is significantly more common in older females than males.^{1,2} Dry eye is also highly prevalent in contact lens wearers.³⁻⁶ There are many clinical tests that can be used to diagnose dry eye. However, a great disparity often exists between the symptoms and signs of dry eye. The diagnostic methods that are often favored by clinicians include patient history, slit-lamp examination and the use of vital dyes, and fluorescein breakup time test. A report of the National Eye Institute/Industry workshop on clinical trials in dry eyes identified several main criteria for diagnosing dry eye,⁷ some of which are difficult to objectively assess in current clinical practice and may be time consuming.⁸

In the lateral shearing interferometer, the cornea is illuminated by a wavefront of approximately 4 mm in diameter, and the information about the tear film surface is enclosed in the shape of the reflected wavefront. The interference is received by the optical wedge.^{9,10} Interferograms present the effect of interference of two subject wavefronts, which are laterally and angularly shifted. Lateral shearing interferometry is one of the most sensitive techniques for recording tear film surface irregularities in a noninvasive manner. At the same time, the technique is hindered by the natural microfluctuations of the eye and small eye movements, which can result in signifi-

cant measurement noise.¹¹ Also, for dry eye patients or contact lens wearers, the pattern of the interference fringes may be significantly disturbed, causing previous techniques for estimating tear film surface quality to fail.^{12,13}

In our previous papers, we introduced the M2 index^{9,10,12} which numerically describes the tear film surface quality (TFSQ) from interferograms. The M2 is calculated based on the second momentum of a general shape of the first harmonic of the Fourier spectrum received from the interferogram. In this paper, we introduce a new method of extracting the first harmonic from the interferogram before the M2 index is computed.

An example of an image acquired under semioptimal conditions for a patient with a normal tear film surface quality is shown in Fig. 1(a). The pattern of the interference fringes in such a case is well defined, and it is easy to estimate its frequency content and, subsequently, relate it to the quality of tear film. Figures 1(b)–1(d) show a blurred frame caused by an eye movement, a frame acquired from a dry eye patient, and a frame acquired from a contact lens wearer where the surface of the lens is almost dry and the interferogram shows a speckled structure, respectively. It is harder to relate the frequency content in those images to the quality of tear film.

Our aim was to develop a technique for estimating tear film surface quality from the interference fringes that would be more robust to the naturally occurring eye movements and the variability in tear film quality encountered in dry eye patients and contact lens wearers. The robustness of the method is not considered here in the statistical Huber sense¹⁴ but in

Address all correspondence to: Dorota H. Szczesna, Wroclaw University of Technology, Institute of Physics, Wyb. Wyspianskiego 27, 50-370 Wroclaw, Poland. Tel: 48-71-320-2592; E-mail: dorota.szczesna@pwr.wroc.pl.

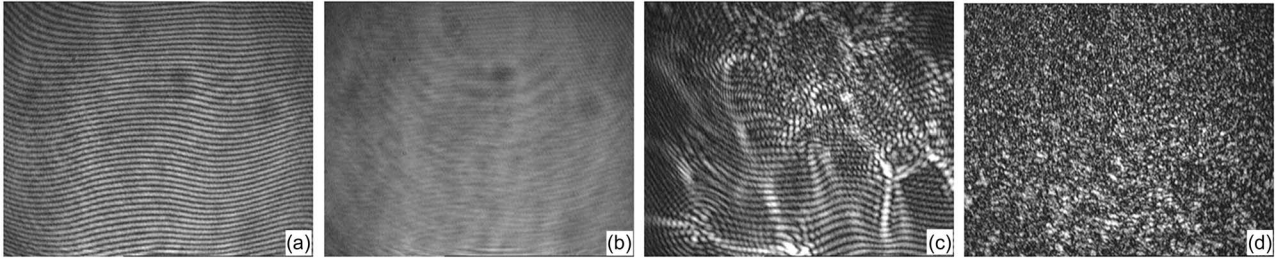


Fig. 1 Examples of interferometric images: (a) a normal patient, (b) blurred frame caused by eye movement, (c) a dry eye patient, and (d) dry surface of a contact lens.

the ability of the method to cope with noisy and strongly disturbed fringe patterns.

2 Methodology

The interferometric method requires a very stable object, which must be positioned at the proper distance from the instrument's lens. The apex curvature of the cornea must overlap the focal point of the lens.¹² The lateral and longitudinal movements of the eye cause disturbance of the reflection of the wavefront. Despite providing a fixation target for the subject, it is hard to avoid small eye movements during the measurement; therefore, their influence on the recorded interferometric images has to be considered in the method of analysis.

The eye movements may lead to interferometric images being only partially covered by fringes, which contain information about the tear film. Hence, in order to analyze the part of the image that is mostly covered by high-contrast fringes, the image that is of size 704×576 is divided into 20 non-overlapping subframes, 128×128 pixels each.^{9,12} Selecting a smaller portion of the interferogram for the analysis also ensures that the observed pattern can be assumed to be stationary.

In the preliminary stage of the procedure, the average intensity in every subframe is calculated across the whole recorded sequence. Those fragments of the image with lower intensity than the empirically chosen threshold are excluded from the analysis. If the number of low-intensity subframes exceeds 65%, the whole image frame is rejected from the analysis. The area of 1/3 of the image as the minimum taken for analysis was chosen empirically in order to capture the early phase of tear film stabilization process (buildup) as well as to eliminate frames captured while the eye moved. Hence, the area of 1/3 of the image is a trade-off between the time resolution of the method immediately after a blink and the robustness of the method to eye movements.

Every subframe is considered as a separate stationary interferogram, $i[m, n]$, $m=1, 2, \dots, M$, $n=1, 2, \dots, N$, $M=N=128$, for which the analysis is applied. The numerical analysis is based on combining the traditional spectral estimation techniques, such as the smoothed periodogram, with morphological image processing techniques, in which the two-dimensional (2-D) spectral content of the interference pattern signal is treated as an image. The periodogram is a maximum likelihood estimator of a sinusoid in noise,¹⁵ so it is chosen here as the first step of analysis:

$$I[k, l] = \frac{1}{MN} \left| \sum_{m=1}^M \sum_{n=1}^N i[m, n] \exp[-j2\pi(km/M + ln/N)] \right|^2, \quad (1)$$

$k=-M/2, -M/2+1, \dots, M/2-1$, $l=-N/2, -N/2+1, \dots, N/2-1$. In the next step, all values below 10% of the maximum of the periodogram $I[k, l]$ are considered as the floor noise and are zeroed, i.e.,

$$I[k, l] = 0 \forall I[k, l] < 0.1 \max_{k,l} (I[k, l]). \quad (2)$$

This step was conducted to remove any spurious local maxima in the periodogram. The 10% threshold has been estimated empirically as a trade-off between the identification of blurred images and high detectability of the first harmonic. The final step in the spectral analysis consists of smoothing the resulted periodogram by convolving it with a kernel function. This is performed to achieve a consistent estimate of the spectral content:

$$\hat{C}[k, l] = \frac{1}{MN} \sum_{p=-M/2}^{M/2-1} \sum_{q=-N/2}^{N/2-1} K(k-p, l-q) I[p, q], \quad (3)$$

where $K(\cdot)$ is a 2-D, symmetric, nonnegative function on the real line. In our application, we chose the 2-D version of the Bartlett-Priestly window for the kernel $K(\cdot)$ because of its optimality property in terms of minimizing the relative mean square error of the estimated spectral density with respect to the functional form of the window.¹⁵

The smoothed periodogram $\hat{C}[k, l]$ is then treated as an image of size $M \times N$ pixels (normalized frequency domain) for which morphological analysis is conducted. In the following, the local maxima of the smoothed periodogram are identified using an 8-connected neighborhood:

$$B[k, l] = \text{local max}(\hat{C}[k, l]), \quad (4)$$

where $B[k, l]$ is a binary (0,1) image, with ones marking the locations of local maxima. The regional maxima are defined as a set of connected pixels that have the same intensity, where external boundary pixels have lower values. This leads to series of estimates of local maxima $\hat{C}_{\max}[k_p, l_p]$, $p=0, 1, \dots, P$, which are further sorted in a descending order, i.e.,

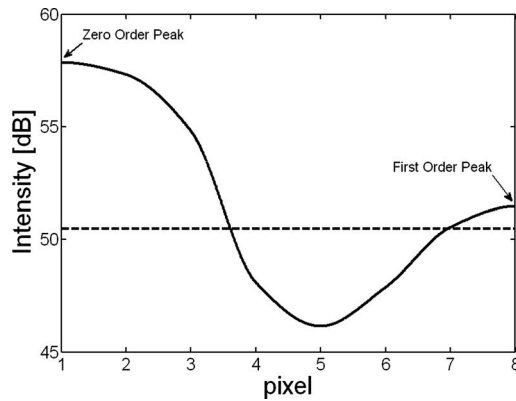


Fig. 2 Example of an oversampled slice of the Fourier spectrum between the zero and the first order of the Fourier spectrum.

$$\hat{C}_{\max}[k_{(0)}, l_{(0)}] \leq \hat{C}_{\max}[k_{(1)}, l_{(1)}] \leq \dots \leq \hat{C}_{\max}[k_{(P)}, l_{(P)}]. \quad (5)$$

The highest local peak value $\hat{C}_{\max}[k_{(0)}, l_{(0)}]$ corresponds to the zero frequency order (the DC value). In the next step, a set of image intensity profiles is sampled from the highest peak $\hat{C}_{\max}[k_{(0)}, l_{(0)}]$ to each of the other estimated peaks $\hat{C}_{\max}[k_{(p)}, l_{(p)}]$, $p=1, 2, \dots, P$.

The nearest-neighbor interpolation is used for computing the slice from the zero order to the local maxima. The minimum absolute value of the pixel in the valley of the profile is compared with the next local maximum. Figure 2 presents an example of the slice between the zero and the first order of the Fourier spectrum. The intensity of pixels is presented in dB scale. The dashed line marks the intensity 1 dB lower than the intensity of the second local maximum. We use the inclusion criterion in which the local maximum is considered as a separate peak provided that the valley between the considered and the zero order peak is below 1 dB.

3 Results

The plots in Fig. 3 present variations of the calculated measure M2 for a subject with normal tear film without blinking during recording (upper row) and a subject with unstable tear film, who blinked two times during recording (bottom row). The original method (left column) and the proposed method (right column) are compared. The values of the M2 index illustrate fast changes in the smoothness of the tear film surface. For the frames of good quality, it is expected that the plot should present a decreasing trend immediately after an eye blink,¹⁶ relatively stable values for the next stage of the tear film kinetics in the case of normal eyes, and increasing characteristic if a breakup appeared in the tear film surface, as is common for dry eye subjects.

In both presented cases, isolated blurred frames caused by a fast eye movement during the recording were present in the sequences. The gaps in the plots indicate that the first harmonics were either not present in the blurred image or they could not have been found in the spectrum in the designated area of analysis.¹²

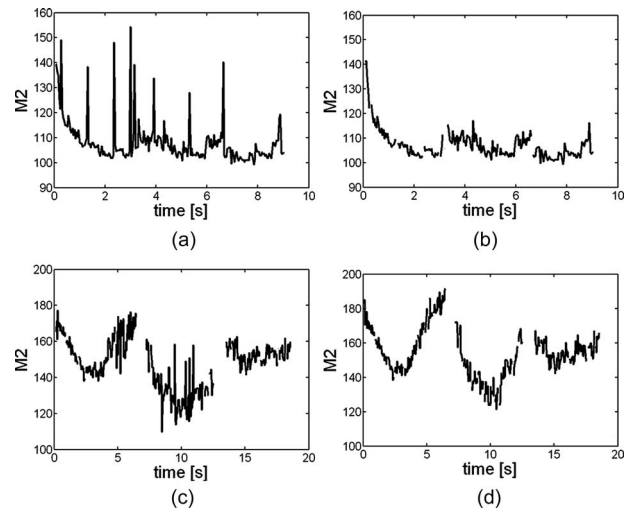


Fig. 3 Examples of plots achieved by using the previous (a, c) and the new (b, d) method of searching the first order in the Fourier spectrum. Upper row: single interblink interval of a normal patient; bottom row: three interblink intervals recorded on a dry eye.

For those blurred frames, for which the first order was found, the M2 value is very high due to spread form of the first harmonics in the spectrum.⁹ As a consequence, the presence of the isolated blurred frames in the sequence manifests in high peaks in the tear film quality indicator as it is presented in Figs. 3(a) and 3(c). Hence, the previous method of computation (of searching for the first order of the Fourier spectrum) required removing the blurred frames from the sequence before the calculation was applied. On the other hand, the proposed method is fully automatic, because there is no need to browse the sequence and remove single frames manually. The plots in Figs. 3(b) and 3(d) were achieved using the new method of searching the first harmonic in the Fourier spectrum. It can be easily seen that the plots are smoother and that they more realistically illustrate the true kinetics of the tear film on the cornea.

4 Discussion

The new estimation technique for extracting the first harmonic from the Fourier spectrum of an interferogram combines the traditional spectral estimation techniques with morphological image processing techniques.

The method of extracting the fragment of the Fourier spectrum for numerical analysis gives a more unambiguous position of the first harmonic. Thus, it gives more robust results in cases of significantly disturbed interference fringes as well allowing the automatic rejection of interferograms of poor quality and contrast.

The zero order of the spectrum is often spread in one specific direction, determined by the tear breakup's shape showing as inhomogeneity of the background of the image.¹⁶ The previous method would require a relatively large mask to cover the zero order. Using the new method, it is much clearer where the first order of the spectrum is located.

If a speckled structure is observed in the interferogram, as in the case of a dry surface of a contact lens, the Fourier spectrum of the image does not present any periodicity, or the

number of the estimated local maxima in the spectrum increases significantly. In the second case, most of such local maxima do not meet the proposed 1-dB condition. No periodical pattern can be noticed then, so no first order of the Fourier spectrum is distinguished.

The new method of extracting the first harmonic also works well in the elimination of blurred images caused by the saccadic movement of the eye. Due to the poor contrast in such images, the first harmonic in the Fourier spectrum is below the floor noise, and after it is cut off, the zero order is the only local maximum in the spectrum. This indicates that the image does not contain information about the tear film surface quality and must be rejected.

The proposed technique gives less noisy results of the tear film surface quality and eliminates the interferograms with poor periodic structure. It is more robust to changes in interference fringes caused by natural eye movements and the degree of dryness of the contact lens and corneal surfaces than its predecessors.

References

1. D. A. Schaumberg, D. A. Sullivan, J. E. Buring, and R. Dana, "Prevalence of dry eye syndrome among US women," *Am. J. Ophthalmol.* **136**, 318–326 (2003).
2. D. A. Schaumberg, R. Dana, J. E. Buring, and D. A. Sullivan, "Prevalence of dry eye syndrome among US men," *Arch. Ophthalmol. (Chicago)* **127**, 763–768 (2009).
3. D. Fonn, P. Situ, and T. Simpson, "Hydrogel lens dehydration and subjective comfort and dryness ratings in symptomatic and asymptomatic contact lens wearers," *Optom. Vision Sci.* **76**, 700–704 (1999).
4. C. G. Begley, B. Caffery, K. K. Nichols, and R. Chalmers, "Responses of contact lens wearers to a dry eye survey," *Optom. Vision Sci.* **77**, 40–46 (2000).
5. M. Guillon and C. Maissa, "Dry eye symptomatology of soft contact lens wearers and nonwearers," *Optom. Vision Sci.* **82**, 829–834 (2005).
6. R. du Toit, P. Situ, T. Simpson, and D. Fonn, "The effects of six months of contact lens wear on the tear film, ocular surfaces, and symptoms of presbyopes," *Optom. Vision Sci.* **78**, 455–462 (2001).
7. M. A. Lemp, "Report of the National Eye Institute/industry workshop on clinical trials in dry eyes," *CLAO J.* **21**, 221–232 (1995).
8. K. K. Nichols, G. L. Mitchell, and K. Zadnik, "The repeatability of clinical measurements of dry eye," *Cornea* **23**, 272–285 (2004).
9. D. H. Szczesna, J. Jaronski, H. T. Kasprzak, and U. Stenevi, "Interferometric measurements of dynamic changes of tear film," *J. Biomed. Opt.* **11**, 34028 (2006).
10. D. H. Szczesna, H. T. Kasprzak, J. Jaronski, A. Rydz, and U. Stenevi, "An interferometric method for the dynamic evaluation of the tear film," *Acta Ophthalmol. Scand.* **85**, 202–208 (2007).
11. A. Dubra, C. Paterson, and C. Dainty, "Double lateral shearing interferometer for the quantitative measurement of tear film topography," *Appl. Opt.* **44**, 1191–1199 (2005).
12. D. H. Szczesna, H. T. Kasprzak, and U. Stenevi, "Application of interferometry for evaluation of the effect of contact lens material on tear film quality," in *Interferometry XIV: Applications*, E. L. Novak, W. Osten, and C. Gorecki, Eds., *Proc. SPIE* **7064**, 706407 (2008).
13. D. H. Szczesna, H. T. Kasprzak, and U. Stenevi, "Interferometric assessment of the efficacy of artificial tears in dry eyes," *Invest. Ophthalmol. Visual Sci.* **49**, E-Abstract 106 (2008).
14. P. J. Huber, *Robust Statistics*, Wiley, New York (1981).
15. M. B. Priestley, *Spectral Analysis and Time Series*, Academic Press, London (1981).
16. D. H. Szczesna and H. T. Kasprzak, "Numerical analysis of interferograms for evaluation of tear film build-up time," *Ophthalmic Physiol. Opt.* **29**, 211–218 (2009).